

LIMITS ON THE ACCRETION RATES ONTO MASSIVE BLACK HOLES IN NEARBY GALAXIES

T. DI MATTEO¹

Harvard-Smithsonian Center for Astrophysics, 60 Garden St., Cambridge, MA 02138; tdimatteo@cfa.harvard.edu

C. L. CARILLI

NRAO, P.O. Box O, Socorro, NM, 87801; ccarilli@aoc.nrao.edu

AND

A. C. FABIAN

Institute of Astronomy, Madingley Road, Cambridge, CB3 OHA, UK; acf@ast.cam.ac.uk

Draft version November 2, 2018

ABSTRACT

The radio emission from supermassive black holes in nearby early-type galaxies can be used to test possible explanations for their low luminosities. We calculate the expected contribution from thermal synchrotron emission from hot accretion flows to the high radio frequency observations of NGC 2300, NGC 1399, NGC 4278 and NGC 4594. We find that, in all cases, and in accordance with our previous findings, hot flows accreting close to their Bondi rates overestimate significantly the observed fluxes. This implies that simply assuming a low radiative efficiency for the accreting gas is not enough to explain their low luminosities. Smaller central densities and accretion rates, as expected in the presence of strong mass loss or convection in the flows, can help reconcile the models with observations. We also show that a significant contribution to the high-frequency radio spectra can be due to non-thermal synchrotron emission from the small scale radio jets observed in these systems, allowing for even lower accretion rates in the inflows. We suggest that these outflows or jets may dump significant energy into the surrounding medium close to the accretion radius and so reduce the accretion rates onto these systems. We discuss the relationship between the radio flux and black hole mass for the observed sample and its potential importance for probing accretion models.

Subject headings: accretion, accretion disks - black hole physics - galaxies: nuclei - radio continuum

1. INTRODUCTION

Most nearby galaxies exhibit little or no nuclear activity. However dynamical arguments based on the observed stellar and gas distributions firmly imply the presence of supermassive compact objects in their cores (Magorrian et al. 1998; Richstone et al. 1999; van der Marel 1999). These studies show that virtually all early-type galaxies host black holes with masses in the range 10^8 – to a few 10^9 M_\odot .

The central black holes in nearby early-type galaxies are probably the remnants of QSO phenomena (McLure et al. 1999). Unlike the giant ellipticals at high redshifts which host radio galaxies and radio-loud quasars, they only display low-luminosity radio cores (Sadler, Jenkins & Kotanji 1989; Wrobel & Heerschen 1991). However, the black holes in the centers of nearby early-type galaxies have enough fuel so that they should still exhibit quasar-like activity. X-ray studies show that they possess extensive hot-gaseous halos which should accrete onto the central black holes and give rise to far more activity than is observed. The Bondi accretion rates for the typical temperatures and densities of their interstellar medium (ISM) are typically estimated to be ~ 0.01 – 0.1 M_\odot yr^{-1} , implying luminosities of 10^{45} – 46 $erg\ s^{-1}$, for standard accretion disks radiative efficiencies of $\sim 10\%$ (see e.g. Di Matteo et al. 2000 for details). Because of the lack of any such activity it has been suggested (Fabian & Rees 1995; Reynolds et al. 1996; Mahadevan 1997; Di Matteo & Fabian 1997,

Di Matteo et al. 1999, 2000 and references therein) that accretion in the nuclei of ellipticals occurs at low radiative efficiency as predicted in advection dominated accretion flow (ADAF) models (e.g. Rees et al. 1982; see Narayan, Mahadevan & Quataert 1998 for a review). In these models, thermal synchrotron emission is predicted to give a strong contribution to the radio emission.

Because the only obvious sign of activity from these supermassive black holes is their radio emission, studies in this band provide a useful tool for constraining accretion models for these systems. In order to discriminate between a potential accretion flow component and emission from the more extended, scaled-down jets, also common around the supermassive black holes in early-type galaxies, it is crucial to examine their core radio emission component at high resolution and high radio frequencies. In previous work we have shown that the high-frequency radio emission from the cores of three elliptical galaxies is strongly suppressed with respect to the standard ADAF model predictions for black holes accreting at close to the Bondi rates (Di Matteo et al. 1999, hereafter DM99). We also showed that radio emission can provide powerful constraints on ADAF models for the cores of ellipticals, implying that the low-radiative efficiency of an ADAF is not enough to explain their low luminosities. and that the accretion rates onto the black holes ought to be smaller than the expected Bondi rates. We have examined how the required suppression can be obtained if strong mass loss is

¹Chandra Fellow

present in hot accretion flows and/or if matter is fed at much lower rates than those expected (DM99). This is in agreement with the proposal that a direct consequence of the dynamics of hot quasi-spherical flows is the development of strong outflows (as emphasized by Begelman & Blandford 1999; Igumenshchev & Abramowicz 1999; Stone, Pringle & Begelman 2000) leading to suppressed density profiles $\rho \propto r^{-3/2+p}$ for $0 < p < 1$ in the flows. For certain regimes, convection might also become important in these hot flows, leading to virtually no accretion and $\rho \propto r^{-1/2}$ (Quataert & Gruzinov 2000; Narayan, Igumenshchev & Abramowicz 2000).

To test how representative our previous results are and how they can constrain the properties of accretion flows in the low luminosity nuclei of nearby early-type galaxies, here we extend our analysis to a larger sample of objects observed at high radio frequencies. We present accretion models based on Very Large Array (VLA) observations at 8, 22 and 43 GHz of four further galaxies, NGC 1399, NGC 2300, NGC 4594, and NGC 4278. We have also re-observed NGC 4649, a Virgo elliptical from our initial sample to test for variability. With the three ellipticals previously studied, we now have seven objects with radio spectra which can be modeled from ~ 5 GHz to 43 GHz.

In the next section we briefly summarize the observations (§2) and in §3 discuss possible accretion and jet models for the observed radio emission (§3). In §4, we derive constraints for hot accretion models. In §5 we discuss how the presence of small-scale radio jets in these systems should heat the ISM close to the accretion radii with a consequent reduction of the accretion rates onto the black holes (independent of any specific consequences of the dynamical properties of hot accretion flows themselves). We also discuss the relationship between radio flux and black hole mass in these objects and show that it can provide a useful tool for constraining accretion flow properties.

2. THE VLA DATA AND THE SPECTRUM OF THE CORE EMISSION

Radio continuum surveys of elliptical and S0 galaxies have indicated that the sources in radio-quiet galaxies tend to show compact components which have relatively flat or slowly rising radio spectra (with a typical spectral index $\alpha \sim 0.3 - 0.4$, where flux, $F_\nu \propto \nu^{-\alpha}$) suggesting that the radio emission from early-type galaxies is, in general, of nuclear origin (Slee et al. 1994; Wrobel 1991).

Our primary goal in obtaining high-frequency, high resolution radio measurements of early-type galaxy radio cores is the determination of their radio spectral energy distributions. This is important because only at high radio frequencies is the inverted-spectrum due to synchrotron radiation from an ADAF (for accretion rates close to the Bondi values) expected to dominate over the flatter spectral component of their compact radio cores. The observation of such an inverted component is crucial for determining the presence of hot-thermal accretion flows around the supermassive black holes in these galaxies and hence for understanding the dominant mode of accretion in these extremely underluminous systems.

Here we use the VLA to extend the sample of objects so far observed at high radio frequencies and present results for NGC 1399, NGC 2300, NGC 4594 and NGC 4278.

Following DM99, in the attempt to resolve the intrinsic spectra of the central point sources of these compact radio cores we obtain flux measurements at 8.4, 22 and 43 GHz. In order to check for core flux variability we have also re-observed NGC 4649 which was the only unresolved point-like source in DM99.

Both NGC 1399 and NGC 2300 have been fairly extensively studied at low radio frequencies and in the X-ray band. NGC 1399 is a giant elliptical at the center of the Fornax Cluster at a distance of ~ 30 Mpc. VLA imaging (6 and 20 cm observations by Killeen, Bickenell & Ekers 1988; and references therein) of NGC 1399 shows that the source is extended with antiparallel jets ($\lesssim 4$ arc min) with small diffuse lobes mostly confined within the extent of the galaxy.

NGC 2300 is an S0 galaxy at a distance of ~ 40 Mpc. Previous VLA observations (Fabbiano, Gioia & Trinchieri 1989) indicate a total flux density of 0.7 mJy at 5 GHz for the source with only upper limits on the flux at 1.4 and 2.4 GHz (Hummel 1980). No radio maps are available.

NGC 4594 is an Sa galaxy at a distance of ~ 10 Mpc with a central black hole mass of $M_{\text{BH}} \approx 2 - 4 \times 10^9 M_\odot$ (Kormendy et al. 1996). It has a prominent bulge with X-ray properties similar to those of E and S0 galaxies (e.g. Fabbiano & Juda 1997). VLA high-resolution data between 0.6 and 15 GHz define a compact flat-spectrum core with α ranging from 0.2 to 0.4 (Hummel, Hulst & Dickey 1984).

NGC 4278 is an elliptical radio galaxy at a distance of 10–13 Mpc (Jacoby et al. 1996; Forbes et al. 1996). Previous 1.4, 5, 15 GHz high-resolution radio measurements of the core spectrum were reported by Wrobel (1991).

2.1. VLA measurements

Observations of NGC 1399, NGC 2300, NGC 4649 were obtained in December 1998, and those of NGC 4594 and NGC 4278 in February 2000 with the VLA at 8.4, 22 and 43 GHz. As an example, in Figure 1 we show the resulting high-resolution radio images for NGC 1399. Data for all the objects are shown in Table 1. In order to obtain the best limits on the core flux for the extended sources, the flux densities, where possible, were derived from images convolved with the resolution of the 8.4 GHz image at all frequencies (seventh column in Table 1). The observations were all made in the VLA C configuration with a maximum baseline of 3 km. The flux scale was set using observations of 3C 286.

NGC 1399: The source is extended at 8 GHz, with prominent twin jets. The companion source to the north east (Fig. 1) has a 11.2 mJy total flux density at 8 GHz, a peak flux of 4.4 mJy at RA 03 38 43.039 and DEC -35 23 40.95 (J2000). It has been identified with an elliptical galaxy (possibly a Seyfert 2) in a cluster behind the Fornax cluster (Killeen et al. 1988; Carter & Malin 1983). The core spectrum of NGC 1399 shows evidence for a slowly rising, high frequency component turning over at ~ 30 GHz (Fig. 2).

NGC 2300: The core of the galaxy is detected with flat/slowly rising spectrum up to 22 GHz, but only at a 4.5σ significance (see contour plots in Fig. 1 and spectrum in Fig. 2). It is not detected at 43 GHz with a 4σ limit of 1.6 mJy.

NGC 4649: In agreement with our previous observations at these frequencies, NGC 4649 is a core dominated source. At 8 GHz, some faint, fuzzy emission to the northeast and a possible jet with a knot at larger distance is observed. The knot has a peak flux of 0.3 mJy and the total flux density of the fuzzy jet emission is 0.77 mJy. The source variability, when compared to our previous observations is less than 15 per cent (see DM99).

NGC 4594: 8, 22 and 43 GHz measurements indicate a fairly steep spectrum for this source (Table 1; Fig. 2). Combining with previous lower frequency observations this implies a spectral turnover at ~ 10 GHz.

NGC 4278: The steep spectral slope (Fig. 2) is likely to be the result of the dominance of emission from the extended jet structures present in this system. This component seems to dominate throughout the radio band and no sharp spectral break is present.

3. MODELS

3.1. ADAFs with/without outflows: thermal models

In a hot accretion flow around a supermassive black hole, the majority of the observable emission arises in the radio and X-ray bands. In the radio band the emission results from synchrotron radiation due to the thermal relativistic electrons moving in the near equipartition magnetic field in the inner parts of the accretion flow. The X-ray emission is due to either bremsstrahlung or inverse Compton scattering of the soft synchrotron photons.

In the thermal plasma of an ADAF the self-absorbed synchrotron emission rises with frequency, ν , roughly as $\sim \nu^{0.3-0.4}$ in the Rayleigh-Jeans limit, up to a critical turnover frequency above which the emission becomes optically thin and drops abruptly. The peak emission always arises from close to the black hole and reflects the properties of the accreting gas within a few Schwarzschild radii. The spectral models with and without outflows and self-consistent temperature profiles which we use here are described in detail in DM00 (and references therein).

The predicted spectrum from an ADAF depends on several microphysics parameters, notably the ratio of gas to magnetic pressure β , the viscosity parameter α , and the fraction of the turbulent energy in the plasma which heats the electrons, δ . Here we fix $\alpha = 0.1$, $\beta = 10$, and $\delta = 0.01$. The two major parameters although, are the accretion rate \dot{M} and the black hole mass M_{BH} .

Models are calculated using the black hole masses reported by Richstone et al. (1998) and Magorrian et al. (1998; second column, Table 1). Following our earlier work, the accretion rates in the flows have been determined from Bondi accretion theory e.g. $\dot{M}_{\text{Bondi}} \propto M_{BH}^2 n(\text{ISM})/c_s(\text{ISM})$ taking ISM densities $n(\text{ISM})$ at a distance of 1 kpc from the centers and sound speeds $c_s(\text{ISM})$, determined from deprojection analysis of the ROSAT HRI data and spectral analysis of ASCA data respectively, for both NGC 1399 (see also Section 2.1 and Table 1 in DM00) and NGC 2300. Because the accretion radii ($R_A = GM_{BH}/c_s^2$) of these systems are typically at ~ 0.1 kpc (with the ISM temperature ~ 1 keV) and the density profile of the hot gas scales as $n(\text{ISM}) \propto r^{-1}$ we extrapolate for the density at $R \sim R_A$. This implies a value of $\sim 0.1 M_{\odot} \text{ yr}^{-1}$ and $\sim 1 M_{\odot} \text{ yr}^{-1}$ for NGC 2300 and

NGC 1399 respectively. For NGC 4594 and NGC 4278 no deprojection analysis is available. The X-ray temperatures of their ISM are estimated to be $kT \sim 0.45$ and 0.5 keV for NGC 4594 (Fabbiano & Juda 1997) and NGC 4278 (Brown & Bregman 1998) respectively. These values are consistent with those of the soft X-ray emission reported for a sample of elliptical galaxies observed with ASCA. For such systems, a deprojection analysis shows that the ISM typically has a density $n(\text{ISM}) \sim 0.1 - 0.5 \text{ cm}^{-3}$ (e.g. Buote & Fabian 1998). Given the black hole masses in Table 1, the Bondi accretion rates for NGC 4594 and 4278 are therefore expected to be $\dot{M} \sim 0.01 - 0.1 M_{\odot} \text{ yr}^{-1}$.

We measure radii in the flow in Schwarzschild units: $R = rR_S$, where $R_S = 2GM_{BH}/c^2$. We measure black hole masses in solar units and accretion rates in Eddington units: $M_{BH} = mM_{\odot}$ and $\dot{M} = \dot{m}M_{\text{Edd}}$. We take $\dot{M}_{\text{Edd}} = 10L_{\text{Edd}}/c^2 = 2.2 \times 10^{-8}m M_{\odot} \text{ yr}^{-1}$, i.e., with a canonical 10% efficiency.

We model the different density profiles (flatter than in the pure Bondi inflow with $\rho \propto r^{-3/2}$) by adopting a mass inflow rate which satisfies: $\dot{m} \propto r^p$. This relation is supported by recent numerical and analytical work (Stone et al. 1999; Igumenshchev et al. 1999; Blandford & Begelman 1999) which has shown that mass loss via winds in hot accretion flows may be both dynamically crucial and quite substantial. In particular, we adopt $\rho \propto r^{-3/2-p}$. We note that for $p = 1$ and $\alpha \lesssim 0.1$, this density profile can also correspond to the case of strong convection; Narayan et al. 2000; Quataert & Gruzinov 2000).

3.2. Jets: non-thermal models

Compact radio cores or scaled down radio jets are also synchrotron emitters. The spectra of compact radio cores are generally flatter than those of extended sources and are often modeled by non-thermal synchrotron radiation from power law distributions of particles. Because of the relative compactness of these sources, synchrotron self-absorption is also often important in this regime. At frequencies low enough for the source to be optically thick, the non-thermal synchrotron spectrum rises as $\propto \nu^{5/2}$ and at frequencies high enough to be optically thin it falls $\propto \nu^{-\alpha}$, where $\alpha = (\xi - 1)/2$ for an electron distribution function $dn/d\gamma \propto \gamma^{-\xi}$, where γ is the Lorentz factor (e.g. Rybicki & Lightman 1979). In between the spectrum has a well-defined peak near a frequency, which, according to standard synchrotron formalism we write as,

$$\nu_t = 2.8 \times 10^6 B \left(\frac{(\xi - 1)f(\xi)e\tau_T}{B\sigma_T} \right)^{2/(\xi+4)}, \quad (1)$$

for which the synchrotron optical depth is unity. Here, τ_T is the electron scattering optical depth across the radius of the source, $f(\xi)$ is given by Blumenthal and Gould (1970) and for $\xi \sim 2 - 3$, $f(\xi) \sim 10$. For compact sources the observed brightness temperature at ν_t can be derived by assuming that the surface brightness is equal to the source function e.g.

$$T_B = 9.3 \times 10^9 \frac{g(\xi)}{f(\xi)} \left(\frac{(\xi - 1)f(\xi)e\tau_T}{B\sigma_T} \right)^{1/(\xi+4)}, \quad (2)$$

where $f(\xi)$ generally $\sim O(1)$ is also given by Blumenthal and Gould (1970). The brightness temperature gives the

energy and hence a typical γ for the electrons radiating at a frequency ν_t ; e.g. $\gamma \sim kT_B/m_e c^2$. Spectra of radio cores do not usually rise as sharply as $\nu^{5/2}$ but their flatter spectral shape can be easily attributed to inhomogeneity. We model the radio spectrum with regions of different optical depth and magnetic field strengths and combine them to reproduce a spectrum that matches the one observed for the different objects over the observed frequencies. A jet provides an extremely natural context for inhomogeneous models. In a jet, because density and magnetic field strength plausibly decline outwards, a number of localized optically thick regions are likely to give rise to the observed emission. From the flux at a frequency ν_t , as given by our VLA observations and using Eq. (1) and (2), we construct simple models for the spectra and deduce approximate optical depths and magnetic field strengths for the given sources.

4. RESULTS: COMPARISON WITH THE DATA

Figure 2 shows our VLA data points and the predicted ADAF self-absorbed synchrotron emission. We note that, as discussed §2.1 and shown in Figure 1, all of the contribution from the weak jets in these systems cannot be ignored and the measured radio fluxes should only be considered as upper limits to the emission from a hot accretion flow in their cores.

Regardless of that and in agreement with our previous results (DM99) we find that in all cases the canonical ADAF model (solid lines in Fig. 2) greatly overestimates the total flux contribution at most frequencies. In addition, although the pure inflow models require the synchrotron emission to peak at $\nu \sim 10^{12}$ Hz, all the objects observed here and in DM99 have spectral energy distributions peaked at $\sim 10 - 30$ GHz, i.e. at energies much lower than predicted by ADAF models.

The emission at the self-absorbed synchrotron peak arises from the inner regions of an ADAF and scales (in the Rayleigh-Jeans limit) as

$$\nu L_\nu \propto \nu_s^2 T_e \propto B^3 T_e^7 \propto \beta^{-3/2} \dot{m}^{3/2} T^7, \quad (3)$$

where \dot{m} is the accretion rate in the innermost regions of the flow. As discussed in DM99 thermal synchrotron emission cannot be suppressed significantly by decreasing the magnetic field strength, B . A decrease in B leads to an increase in the flow temperature and hence an increase in synchrotron cooling itself (unless B is reduced to values below 0.1% equipartition; see Eq. 3 and DM99). In addition, the lack of any significant variability of the high frequency emission from the most point-like source in our sample, NGC 4649 (Table 1), and the faint high frequency radio fluxes systematically observed in all seven sources, excludes the possibility that significant variability may be the cause of the lack of the high energy radio flux.

However, if the accretion rates in the inner regions of an ADAF (where all of the high energy emission is produced; see Eq. (3)) are decreased with respect to the Bondi values discussed in §3.1, the ADAF models can be brought to agreement with the data. There are two ways this can be achieved (see also DM99). The presence of mass loss implies $\dot{m} \propto r$ which can lead to significant suppression of the central densities and accommodate the observed lack of a

high energy synchrotron component (in particular because the electron temperature T_e also decreases as p increases giving rise to a steep decrease in the synchrotron component; Eq. 3). An alternative possibility is that the gas is not fed to flows at the expected Bondi rates (see §5.1 and Di Matteo & Fabian 2000) and \dot{m} is much smaller than estimated in §3.1 or in previous work (but possibly consistent with values deduced directly from the lower frequencies radio flux; e.g. Wrobel & Herrnstein 2000).

Spectral models which include strong mass loss are shown by the long dashed lines in Fig. 2. For these models we adopt an accretion rate which satisfies $\dot{m} = \dot{m}_{\text{Bondi}}(r/r_{\text{out}})^p$. For NGC 2300 the dashed line is for $\dot{m}_{\text{Bondi}} = 2.6 \times 10^{-3}$, $r_{\text{out}} = 300$ and $p = 0.68$. For NGC 1399 we used $\dot{m}_{\text{Bondi}} = 10^{-2}$, $p = 0.78$ and $r_{\text{out}} = 220$. For NGC 4594 $\dot{m}_{\text{Bondi}} = 3 \times 10^{-3}$, $p = 0.5$ and $r_{\text{out}} = 300$. We use $m = 4 \times 10^9$ to fit the low frequency radio data. Finally for NGC 4278 $\dot{m}_{\text{Bondi}} = 2 \times 10^{-3}$, $p = 0.4$ and $r_{\text{out}} = 200$. We note that similar fits (but with slightly steeper rising spectra) are obtained with $p \sim 1$ and $R_{\text{out}} \sim 10^4$, corresponding to the full extent of the flow.

In all of the above cases, the values of p and r_{out} imply that only a few percent of the Bondi mass accretion rates are actually accreted onto the black holes and that most of the mass is lost in the outflows

In Figure 2 we also show models for which \dot{m} is again constant but $\ll \dot{m}_{\text{Bondi}}$ (short dashed lines) so as to agree the radio limits. We find that values of $\dot{m} \lesssim$ a few $\times 10^{-5}$ ($\lesssim 10^{-2} \dot{m}_{\text{Bondi}}$) are consistent with the radio measurements. We note that for these low accretion rates the temperature profiles steepen causing the slope of the synchrotron component also to steepen. As a result, the radio fluxes are fitted less well by these models and definitely require an additional more extended component (most likely the jets) to account for a significant fraction of the observed fluxes.

In Figure 3 we also model the radio spectra of the four galaxies by non-thermal synchrotron emission from compact 'jet-like' regions as described in §3.2. In the ADAF models, we have assumed that there is no contribution to the observed emission from either the outflows (which are considered non-radiative) or from compact regions in the scaled-down radio jets also present in these sources. Here we test whether non-thermal synchrotron models can also explain the radio spectral energy distributions and/or whether the physical parameters they require may favor the hot-accretion flow interpretation. Figure 3 shows that if the accretion rates in an ADAF are indeed stifled, either in the inner regions or throughout the hot flow such as is implied by our findings above (or if indeed these systems are accreting via standard thin disks at even lower accretion rates), the radio data can be easily explained by standard non-thermal models for compact radio sources.

If we adopt the hypothesis of inhomogeneity (§3.2), the observed spectral breaks in the different sources and the general spectral shapes can be modeled simply by the emission from different compact regions emitting self-absorbed non-thermal synchrotron emission. In order to reproduce the steep fall off above 10 – 30 GHz for most objects or indeed the typically steep, non-thermal spectrum of NGC 4278 we take $\xi = 3$. To infer rough values of optical depths and magnetic field strengths in the different re-

gions we designate the frequencies ν_t and use the brightness temperatures and (upper limits for) the sizes implied by our VLA measurements at the appropriate frequencies. We then use Equations (1) and (2) and the models shown in Figure 3 and infer $B \sim 7 \times 10^{-4} \nu_t \text{GHz} T_{B12}^{-2} \text{ G}$ and $\tau_T \sim 0.4 T_{B12}^5 \nu_t \text{GHz}$, which are typical values for core dominated, synchrotron self-absorbed sources. We note that the models in Figure 3 are not unique (different particle distributions and different regions can be used) but they provide fairly solid estimates for the ranges of parameters that characterize the sources, and imply that the electrons we see directly have $\gamma \sim$ a few 100. Similar models have been constructed to model the radio spectral energy distribution of Sgr A* and other galactic radio cores (e.g. Falcke & Biermann 1999; Beckert & Duschl 1997).

5. DISCUSSION

We have found that all of the seven galactic radio cores observed here and in DM99 show severe discrepancies with the ADAF model predictions. Independent of its actual origin, the observed radio flux is always much less than that expected from pure inflow ADAFs accreting close to their Bondi accretion rates. Even in those objects where a spectral turnover is observed, as expected from thermal synchrotron emission from these hot accretion flows, it is usually at frequencies $\nu \sim 20 - 30 \text{ GHz}$, much lower than those predicted from ADAF models. We have examined the constraints imposed on ADAF models by the high-frequency radio observations.

We have shown that, if indeed these supermassive black holes accrete via hot accretion flows, the suppression of the synchrotron component (in agreement with the radio observations), implies that the accretion rates onto the central black holes ought to be greatly reduced with respect to the Bondi rates estimated from the temperature and density of the hot ISM. One way we can accommodate the lower accretion rates is by including strong mass loss/winds in the hot accretion flows. This is equivalent to adopting density profiles in the flows which are flatter than those for a pure inflow ADAF; with $\rho \propto r^{-3/2+p}$ (see §4 and Fig. 2). The presence of outflows (as proposed by Blandford & Begelman 1999) is strongly supported by numerical simulations (Stone et al. 1999; Igumenschev et al. 1999; 2000) showing that mass loss can be a dynamical consequence of accretion occurring in these regimes. Recent work also emphasizes that convection (when $\alpha \lesssim 0.1$) may also lead to significantly suppressed densities in the inner regions of hot flows (Narayan et al. 2000; Quataert & Gruzinov 2000) with almost no accretion onto the black holes and $\rho \propto r^{-1/2}$. In addition to the above explanations, which are based on the possible consequences of the internal dynamics of a hot/quasi-spherical accretion flow, there may also be processes that simply change the physical conditions in the ISM in regions close to the accretion radii of the systems such that small amounts of material are fed to the flows (§5.1). Any such process would need to reduce \dot{m} by a factor ~ 100 with respect to the estimated Bondi rate (Section 4, Fig. 2).

We have also shown that given the observed low radio flux densities (and given the resolution of the VLA) even

the high-frequency radio emission from these nuclei can be easily reproduced by standard models of self-absorbed non-thermal synchrotron emission from the small scale radio jets observed in these systems (Fig. 3). This implies that the derived \dot{m} (and/or p values in the case of winds) can only provide upper limits to the possible contribution from hot accretion flows and that the relevant accretion rates could feasibly be lower. The radio emission could be produced in localized regions in the outflows/jets where the radiative efficiencies are much higher. If \dot{m} is small enough, a hot accretion flow may not even be required and accretion could for example occur via a standard accretion disk with high radiative efficiency with extremely low accretion rates (to satisfy $L \sim 0.1 \dot{M} c^2$) ¹

It is important to note that the standard ADAF model is also inconsistent with the recent detection of linear polarization (Aitken et al. 2000) at 1mm in Sgr A*. A standard ADAF model is unpolarized at these frequencies. In accordance with the constraints we have obtained here for the elliptical galaxy cores, in Sgr A* the accretion rate has to be much lower than that expected from Bondi estimates (Agol 2000; Quataert & Gruzinov 2000).

We propose that the small-scale radio jets present in these systems may heat the gas in the ISM close to the accretion radii of these systems and stifle the accretion.

5.1. Low \dot{m} : Heating at the accretion radius by outflows/jets

We suggest that outflows may stifle accretion by reducing \dot{M} . The small scales radio jets, present in all of these systems (which may or may not be dynamically coupled to a hot accretion flow), are likely to transfer momentum and energy to the ambient gas. Because the sizes of the radio jets are similar to those inferred for the accretion radii of these systems, (see §3; for the black hole masses of $\sim 10^9 M_\odot$) the radio jets may heat the ISM gas in that region. If gas outside and around the accretion radius, R_A , is heated, the accretion radius decreases (potentially up to a point where the accretion radius may not even exist) leading to a decrease in the accretion rate (or luminosity), where $\dot{m} \propto R_A^2 \rho(R_A) c_s(R_A) \propto T^{-5/2}$, for a given external pressure (see Di Matteo & Fabian 2000 for details). Given that small scale radio jets are observed in basically all early type galaxy cores, we may expect the accretion rates to be reduced in most cases. The heating of the ISM by jets/outflows may lead to similar effects as those due to conduction (Gruzinov 1999), possibly induced by the presence of high magnetic fields which build up in the central regions of the hot, cooling ISM.

We note that if the accretion rate is indeed regulated by jet activity we should expect these sources to undergo cycles of activity. As the jets heat up the ISM we expect the the accretion rates to decrease, but such a decrease will most likely lead to a decline of the jet activity itself. As the heating of the ISM is then suppressed one might expect the fueling onto the central object to be resumed. With the increased accretion rates and luminosities the cycle can be started again.

¹A pure Bondi accretion flow would also have even lower radiative efficiencies than an ADAF and therefore may also be relevant, although it would be hard to reconcile the absence of any angular momentum in the flow and the presence of jets in these systems.

5.1.1. Jets and ISM pressure

Although at lower frequencies (i.e. at larger scales) the thermal pressure of the hot X-ray gas (often forming a cooling flow) may be enough to confine the radio sources (e.g. Fabbiano et al. 1987; 1988) the core regions of the jet are likely to be overpressured with respect to the X-ray gas (see e.g. Fig.1, where the larger scale emission seems to have been disrupted by the cooling ISM gas at low frequencies and only expanding buoyantly through the medium)². Taking the estimates of B from §4, we expect $P_B \sim \text{a few} \times 10^{-10} \text{ dyn cm}^{-2}$ in the jets. The pressure in the X-ray gas, $P_x \sim nkT \sim \text{a few } 10^{-11} \text{ dyn cm}^{-2}$ for central gas densities $n(\text{ISM}) \sim 0.1 - 0.4$ and typical temperatures $kT \sim 1 \text{ keV}$ (DM00). Simple estimates of the energetics of the core also suggest that significant power from the radio source has been deposited in the inner X-ray gas. The rate of energy supplied to the ISM is greater than just the radio luminosity, $L_{\text{radio}} \sim \nu_{\text{max}} L_{\nu_{\text{max}}} \sim 10^{38-39} \text{ erg s}^{-1}$, and is at least $L_j \sim L_{\text{radio}}(D/r)(c/v_j) \sim 100 L_{\text{radio}}$ where $D/r \gtrsim 10$, is the ratio of jet distance from the central object (D) to its radius r and v_j/c , the ratio of the jet to light speed, is typically $\lesssim 0.1$ for these weak sources. The bolometric luminosity of the X-ray gas within $\sim 1 \text{ kpc}$ (which is often greater than the extent of the jets) in the galaxies, $L_x \sim 10^{40-41} \text{ erg s}^{-1}$ (e.g., Allen et al. 2000) is $\sim L_j$, suggesting that the jet power has a strong effect on the thermal balance of the X-ray gas. Note that although it is unclear whether the jets can heat most of the gas (and not just a small fraction of it) near the accretion radii of the systems, if the jets are overpressured with respect to the ISM gas we expect that they will be widening sideways as they drive the shock into the surrounding gas and may therefore affect a large area (Begelman & Cioffi 1990).

5.2. Suppressed accretion rates or mass loss

In both of the models discussed in §4 the accretion rates onto the central black holes in early-type galaxies must be reduced with respect to the Bondi estimates. The low radiative efficiencies of ADAFs are not enough to explain their low-luminosities. If mass loss is important, the accretion rates may only be reduced in the inner regions of the flows and the material may still be fed at the expected Bondi rates in the outer regions, for a fixed temperature and density of the ISM. If instead the ISM is heated near the Bondi radius the accretion rate may be suppressed at large radii and $\dot{m} \ll \dot{m}_{\text{Bondi}}$ throughout the flows.

Follow-up X-ray observations will provide means for distinguishing between these two possibilities. As discussed in detail in DM00, models with strong mass loss (winds) predict significant X-ray fluxes due to bremsstrahlung emission. Most of the contribution to the bremsstrahlung luminosity comes from the outer regions of the flows where the accretion rate is high and the densities are also relatively high (see e.g. Figure 2 in DM00). If \dot{m} is suppressed because jets/outflows heat the ISM significantly in the outer regions of the flow, we expect the bremsstrahlung emission, which is $\propto \rho^2$, to be strongly reduced by a factor $\sim (\dot{m}/\dot{m}_{\text{Bondi}})^2$. Note that because of the low L/L_{Edd} ratios in these sources ($\lesssim 10-5-6$), even if accretion was

to occur via a standard thin disk the dominant X-ray emission mechanism would most likely be bremsstrahlung.

We have argued that the 2 – 10 keV ASCA hard X-ray power laws detected in a number of nearby ellipticals (Allen et al. 2000), if indeed produced by accretion around their central black holes, favors strong outflow models (DM00). Observations with the Chandra X-ray observatory are needed to clearly resolve the central sources in these objects. At present, because of the lack of a clear detection of nuclear X-ray emission, it is not possible to exclude the possibility that the accretion rates in these systems are simply much lower than those implied the Bondi estimates.

Higher resolution VLBA observations at high radio frequencies for $M_{\text{BH}} \sim 10^9 M_{\odot}$ should resolve scales as small as a few tens of R_S and would therefore provide a crucial test for the presence of hot accretion flows in these systems. Results from 15 GHz VLBA imaging (Falcke et al. 1999) of a sample of galaxies (both ellipticals and spirals) show that many radio cores may still be of non-thermal origin. Further observations at higher frequencies are necessary to clearly determine the spectrum of the core emission.

The relationship between the high-frequency radio flux and the estimated black hole masses can also provide some clues for explaining the quiescence of these systems. Franceschini et al. (1998) have shown that there is a direct relation between the 5 GHz radio cores in ellipticals and their central black hole masses, which may be accounted for by the thermal synchrotron emission from an ADAF. If such a proposal is valid and a low- \dot{m} ADAF (Fig. 2) is indeed producing most of the emission, the relationship should hold at higher frequencies. In the next section we derive the expected relationship when outflows are present or when heating of the ISM is occurring.

5.3. Radio power and black hole masses

The high frequency radio observations have allowed both the synchrotron flux and the position of the peak, if present, to be measured. In Figure 4 we plot the radio luminosity at 8 and 22 GHz versus the measured black hole masses for the seven objects (from DM99 and the four here). Although the sample is small and only spans a limited range of black hole masses, much smaller than that plotted in Franceschini et al. (1998), we can still compare our results to the relationship they have found. This allows us to see whether the Franceschini et al. relationship holds at higher frequencies where the contribution from a potential ADAF is most relevant. We also show that the presence of outflows in an ADAF or of significant heating in the ISM, would change the relationships between radio core flux and black hole masses.

Figure 4 shows the radio core luminosities and total radio luminosities for NGC 4649, NGC 4472, NGC 1399, NGC 2300, NGC 4594, NGC 4278 and M87 plotted against their black hole masses. We plot the fluxes measured at 8 and 22 GHz together with the previously reported 5 GHz values (we do not plot the 43 GHz fluxes because at this frequency we only have firm detections for 4 objects). The relationship depicted from the fluxes measured at 22 GHz (solid dots - Figure 4) suggests that the high frequency core fluxes may be more strongly correlated to M_{BH} . Note

²This may also suggest that these sources may be relatively young, also suggested by their fairly peaked spectral distribution

that the 5 GHz fluxes, would indicate a much flatter relationship between M_{BH} and L_{ν} . This suggests that the relatively weak, arcsec-scale radio jet components, which contribute more predominantly at lower frequencies may not be as strongly correlated in this plane.

In Figure 4 we also show the expected correlation (solid line) between radio luminosity and black hole mass for an ADAF (dashed line; Franceschini et al. 1998) and for an ADAF with winds (dotted line). This relationship is obtained by noting that the Rayleigh Jeans part of the synchrotron spectrum scales as $L_{\nu_c} \propto \nu_c^2 R^2$ with $\nu_c \propto B \propto R^{-5/4} \dot{M}^{1/2} M_{\text{BH}}^{1/4}$. For $\dot{M} \propto \dot{M}_{\text{Bondi}} R^p$ we have

$$R \propto \nu_c^{4/(-5+2p)} \dot{M}_{\text{Bondi}}^{2/(5-2p)} M_{\text{BH}}^{1/(5-2p)} \quad (4)$$

and given that $\dot{M}_{\text{Bondi}} \propto M_{\text{BH}}^2 n(\text{ISM})/c_s^3(\text{ISM})$ and following Franceschini et al. (1998) taking $n \propto M_{\text{gal}}$ and $c_s \propto M_{\text{BH}}^{1/4}$ with $M_{\text{gal}} \propto M_{\text{BH}}$ for ellipticals (e.g. Magorrian et al. 1998), we find, using Eq. (4),

$$L_{\nu} \propto \nu_c^{(4p-2)/(2p-5)} M_{\text{BH}}^{11/(5-2p)} \quad (5)$$

which recovers $L_{\nu} \propto \nu^{2/5} M_{\text{BH}}^{2.2}$ derived by Franceschini et al. for the case of $p = 0$. Relation (5) implies that the presence of outflows i.e. for $0 < p \lesssim 1$ steepens the relationship between core power and black hole mass. The solid line in Figure 4 is the steep correlation $L_{\nu} \propto M_{\text{BH}}^{3.6}$ obtained for $p = 1$. A few of the objects seem in better agreement with the steeper relationship, although a larger number of objects would be needed to distinguish any clear trend. Note also that in their regression analysis for 8 objects, Franceschini et al. found $L_{\nu} \propto M_{\text{BH}}^{2.66-2.73}$ for the total and core radio luminosities respectively.

We note that Franceschini et al. (1998) also plot objects like M31 and Sgr A* and their relationship extends down to $M_{\text{BH}} \sim 10^6 M_{\odot}$. Here we could also plot higher frequency radio measurements of those objects (and e.g. NGC 4258) but for those systems Bondi accretion from the ISM would not apply as indicated by Eq. 8 and the expected relationship may be flatter with $L_{\nu} \propto \dot{m}^{6/5} M_{\text{BH}}^{8/5}$. Relation (5) is only recovered where the Bondi argument for the accretion rates can be applied.

The other possibility discussed above is that outflows stifle the accretion by reducing \dot{M} . This could be both due to the possibly poorly collimated outflows from the ADAF or in any case to the observed radio jets present in all these systems. In this case we predict a different relationship between radio power and mass accretion rate.

Heating of the gas at the accretion radius implies an effective energy flux into the ISM and a relationship with the central black hole mass given by,

$$L_{\text{j}} \propto \dot{M} T(\text{ISM}) \propto M_{\text{BH}}^3/c_s(\text{ISM}) \propto M_{\text{BH}}^{2.75}. \quad (6)$$

Given that $L_{\text{j}} \propto L_{\text{radio}}$ if heating by the jets is important we would also expect a strong dependence of the total radio power on the central black hole mass. In Figure 5 we plot the radio power $\nu_{\text{max}} L_{\nu_{\text{max}}}$ versus black hole mass. Although the errors on the black hole mass estimates are not well-known and could easily be large, Fig. 5 seems to show a more consistent trend than Figure 4. The two most powerful radio sources in the sample, NGC 4278 and M87, are the ones that depart the most from the above relation.

In summary, Figure 4 and 5 suggest that the radio power at high radio frequencies is likely to be a good tracer of black hole mass and useful for testing the accretion properties of these systems. The Franceschini et al. relationship between core radio power and black hole mass may get steeper at higher frequencies or in the presence of outflows.

Obtaining a large enough sample of elliptical galaxies observed at high resolution at high radio frequencies spanning a larger range of measured black hole masses may be useful for discriminating whether the radio emission is due to the weak radio jets in these systems or an ADAF component. In particular, with a statistical sample of objects one can test for the presence of strong outflows in ADAFs, or look for signs of interactions between jets and ISM, which can lead to suppression of the accretion onto these systems. Resolving the correlation between black hole mass and radio flux can therefore break the degeneracy between the two interpretations for the origin of the radio emission: the case for small accretion rates throughout the flows (i.e. the case where \dot{M}_{Bondi}) or the situation where most of the material is lost through a wind and small amounts are accreted onto the black holes, $\dot{M} \propto \dot{M}_{\text{Bondi}} R^p$.

T. D. M. acknowledges support for this work provided by NASA through Chandra Postdoctoral Fellowship grant number PF8-10005 awarded by the Chandra Science Center, which is operated by the Smithsonian Astrophysical Observatory for NASA under contract NAS8-39073. ACF thanks the Royal Society for support. The Very Large Array is operated by the National Radio Astronomy Observatory, which is a facility of the National Science Foundation operated under cooperative agreement with Associated Universities Inc.

REFERENCES

- Agol, E., 2000, ApJ, submitted, (astro-ph/0005051)
 Allen S.W., Di Matteo T., Fabian A.C., 2000, MNRAS, 311, 493
 Beckert T., Duschl, W. J., 1997, A&A, 328, 95
 Begelman M. C., Cioffi D.F., 1990, ApJ, 345, L21
 Blandford R.D., Begelman M.C., 1999, MNRAS, 303, L1
 Di Matteo T., Fabian A.C., 1997, MNRAS, 286, 393
 Di Matteo T., Fabian A.C., 2000, in preparation
 Di Matteo T., Fabian A.C., Rees M.J., Carilli C., Ivison R. J., 1999, MNRAS, 305, 49 (DM99)
 Di Matteo, T., Quataert, E., Allen, S. W., Narayan, R. Fabian, A. C. 2000, MNRAS, 311, 507 (DM00)
 Fabian A. C., Canizares C. R., 1988, Nat, 333, 829
 Fabian A. C., Rees M. J., 1995, MNRAS, 277, L55
 Fabbiano G., Juda J.Z., 1997, ApJ, 476, 666
 Falcke H., Biermann, P.L., 1999, A&A, 342, 49
 Falcke H., Nagar N.M., Wilson A.S., Ho L.C., Ulvestad J.S., 2000, ApJ, in press (astro-ph/0005383)
 Forbes, D. A. 1996, AJ, 112, 1409
 Franceschini A., Vercellone S., Fabian A.C., 1998, MNRAS, 297, 817
 Hummel E., van der Hulst J.M., Dickey J.M., 1984, A&A, 134, 207
 Igumenshchev, I. V. Abramowicz, M. A. 1999, MNRAS, 303, 309
 Killeen, N.E.B., Bicknell G. W., Ekers R. D., 1988, ApJ, 325, 180
 Kormendy et al., 1996, ApJ, 473, L91
 Magorrian J. et al., 1998, AJ, 115, 2285

- McLure, R. J., Kukula, M. J., Dunlop, J. S., Baum, S. A., O'Dea C. P., Hughes D. H., 1999, MNRAS, 308, 377
- Mahadevan R., 1997, ApJ, 477, 585
- Narayan R., Yi I., 1995, ApJ, 444, 231
- Narayan R., Igumenshchev, I. V. Abramowicz, M. A., 2000, ApJ, in press (astro-ph/0004006)
- Narayan, R., Mahadevan, R. & Quataert, E. 1998, in Theory of Black Hole Accretion Disks, Eds. M. Abramowicz, G. Bjornsson, and J. Pringle (Cambridge: Cambridge University Press)
- Quataert E., Gruzinov I., 2000, ApJ, in press, (astro-ph/9912440)
- Quataert E., Gruzinov I., 2000, ApJ, submitted, (astro-ph/0004286)
- Quataert E., Narayan R., 1999, ApJ, 520, 298
- Rees M. J., 1982, in Riegler G., Blandford R., eds, The Galactic Center. Am. Inst. Phys., New York, 166
- Rees M. J., Begelman M. C., Blandford R. D., Phinney E. S., 1982, NAT., 295, 17
- Reynolds C. S., Di Matteo T., Fabian A. C., Hwang U., Canizares C. R., 1997, MNRAS, 283, L111
- Richstone et al., 1998, Nature, 395, 14
- Sadler E. M., Jenkins C. R., Kotanji C. G., 1989, MNRAS, 240, 591
- Slee O. B., Sadler E. M., Reynolds J. E., Ekers R. D., 1994, MNRAS, 269, 928
- Stone, J. M., Pringle, J. E. Begelman, M. C. 1999, MNRAS, 310, 1002
- Wrobel J. M., 1991, AJ, 101, 127
- Wrobel J. M., Heeshen D.S., 1991, AJ, 101, 148
- Wrobel, J. M., Herrnstein, J. R., 2000, ApJ, 533, L111
- Van der Marel R.P., 1999, AJ, 117, 744

Table 1: VLA data.

Object	Black Hole	Frequency	RMS	Total	Peak	Peak		Position
						F_ν (mJy)	F_ν (mJy)	
NGC 1399	5.2×10^9	8.4	0.05	159	21.6 ± 0.4	21.6 ± 0.4	03 38 29.0 -35 27 01.0	
		22	0.30	59	22.2 ± 1.2	25.4 ± 1.5	03 38 29.0 -35 27 00.8	
		43	0.7	19	16.1 ± 1.6	17.9 ± 2.0	03 38 29.0 -35 27 01.1	
NGC 2300	2.7×10^9	8.4	0.05	0.76	0.76 ± 0.05	–	07 32 20.2 +85 42 32.5	
		22	0.25	1.5	1.2 ± 0.25	–	07 32 19.9 +85 42 32.6	
		43	0.4	–	< 1.3	–	07 32 20.7 +85 42 27.6	
NGC 4649	3.9×10^9	8.4	0.05	22.7	20.4 ± 0.4	20.4 ± 0.4	12 43 39.96 +11 33 09.8	
		22	0.25	20.7	19.7 ± 1.0	20.4 ± 1.0	12 43 39.97 +11 33 09.6	
		43	0.38	15.9	14.5 ± 1.4	16.2 ± 2.0	12 43 39.97 +11 33 09.7	
NGC 4594	2×10^9	8.4	0.53	137 ± 2.7	136 ± 2.7			
		22	0.41	93 ± 4.6	90.4 ± 4.5			
		43	0.76	57 ± 6	53 ± 5			12 39 59.4 -11 37 23.0
NGC 4278	1.6×10^9	8.4	0.20	133 ± 2.6	129 ± 2.6			
		22	0.26	67 ± 3.3	65 ± 3.2			
		43	0.31	51 ± 5	50 ± 5			12 20 06.8 29 16 50.8

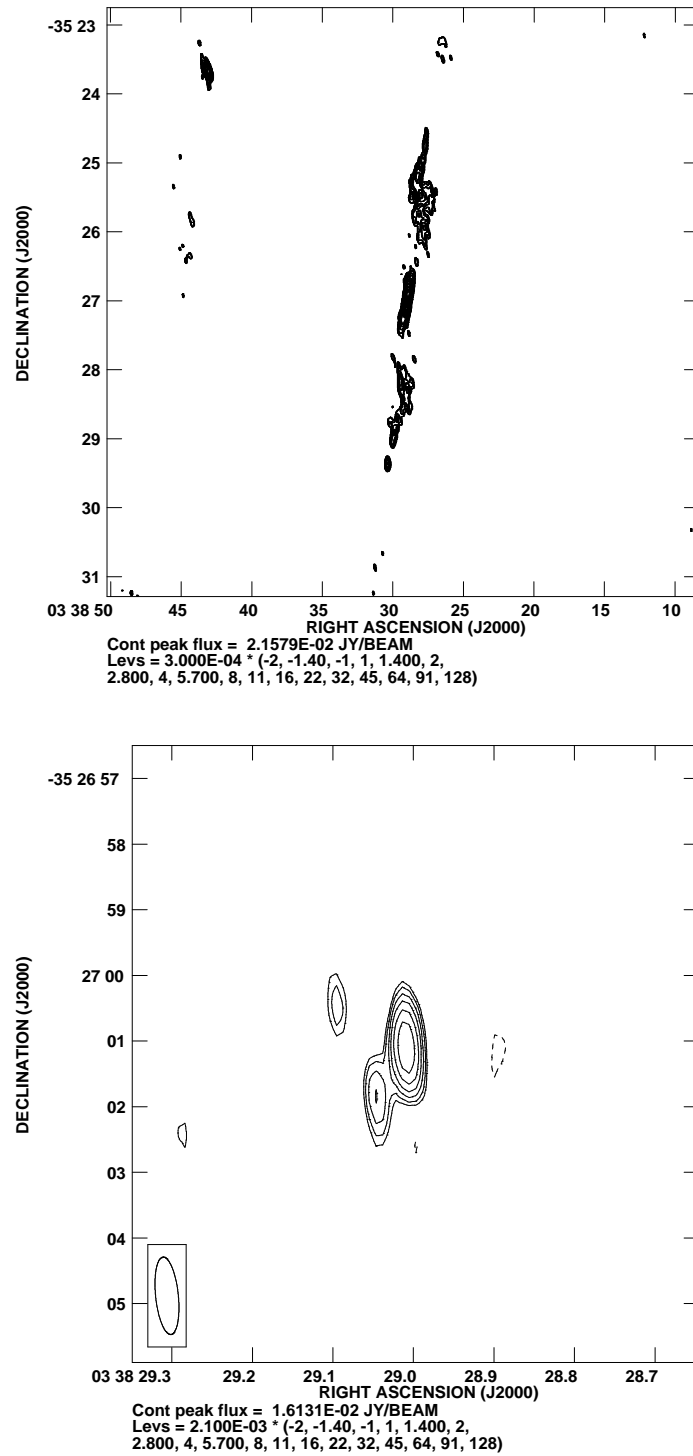


Fig. 1.— VLA high resolution radio images for NGC 1399 at 8 and 43 GHz. The FWHM of the restoring Gaussian beam is shown in the box in lower left corner.

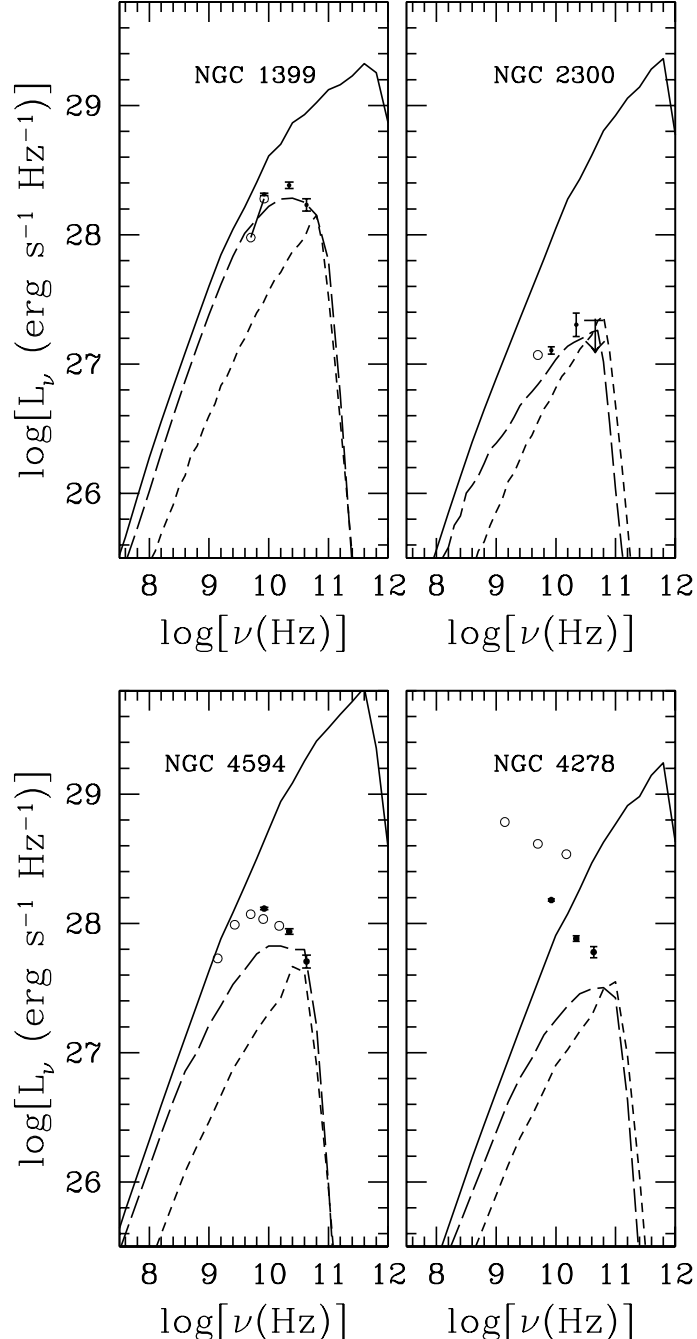


Fig. 2.— The thermal synchrotron emission spectra from hot accretion flows with and without outflows. The solid dots are the VLA fluxes from Table 1. The open circle measurements obtained from literature. The solid line shows pure inflow ADAF models with $\dot{m} \sim \dot{m}_{\text{Bondi}}$, the long dashed lines models with strong outflows $\dot{m} \propto \dot{m}_{\text{Bondi}} r^p$ and the short dashed lines ADAF models without outflows but with $\dot{m} \ll \dot{m}_{\text{Bondi}}$.

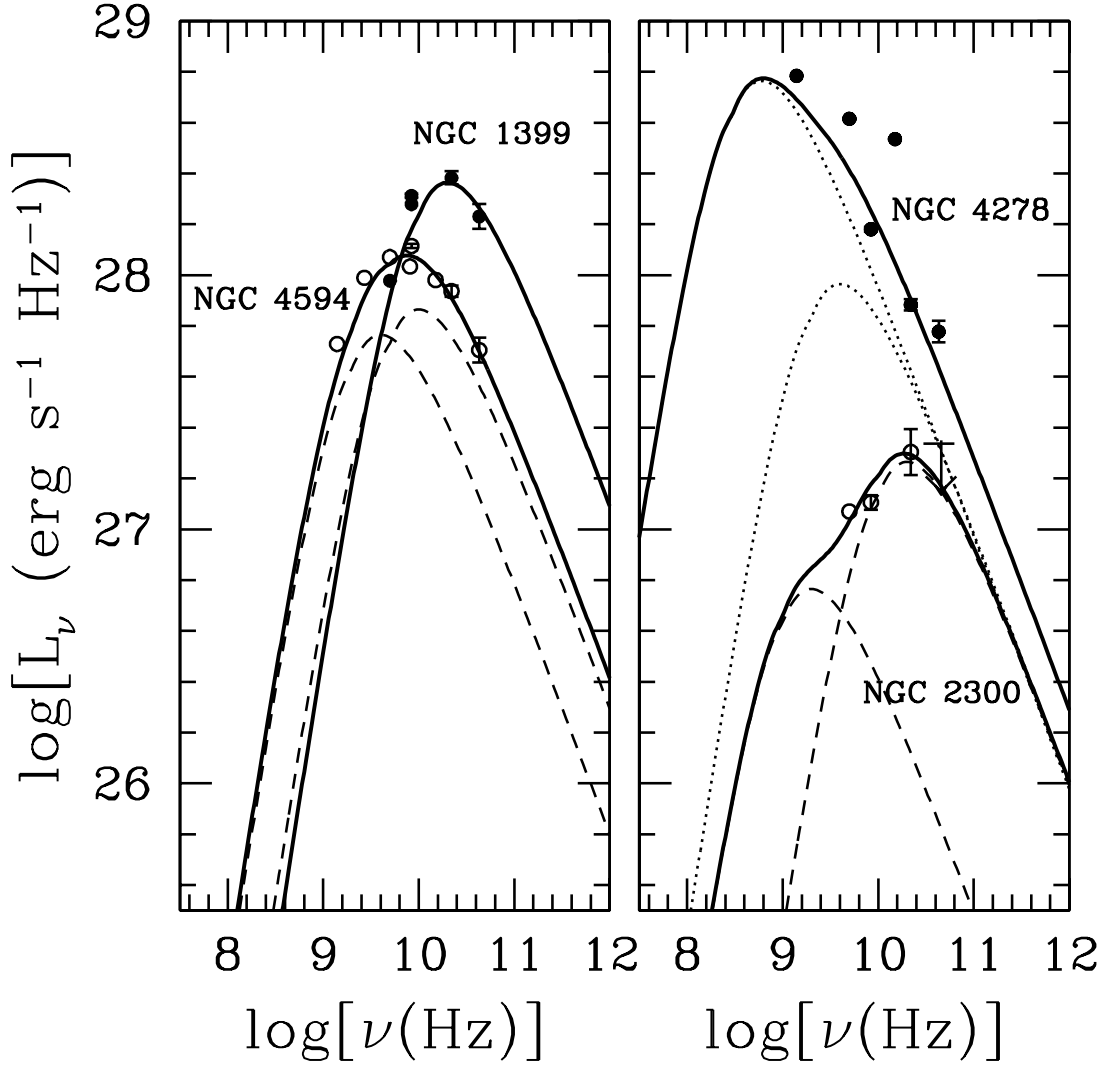


Fig. 3.— Spectra made by superposition of non-thermal self-absorbed synchrotron regions. The solid lines are the sum of the various components the dashed lines and dotted lines show the separate components. At these frequencies NGC 4594 can be well-explained with only one region. For the other objects two-regions are modeled. All models have $\xi = 3$. The data points are the same as in Figure 2.

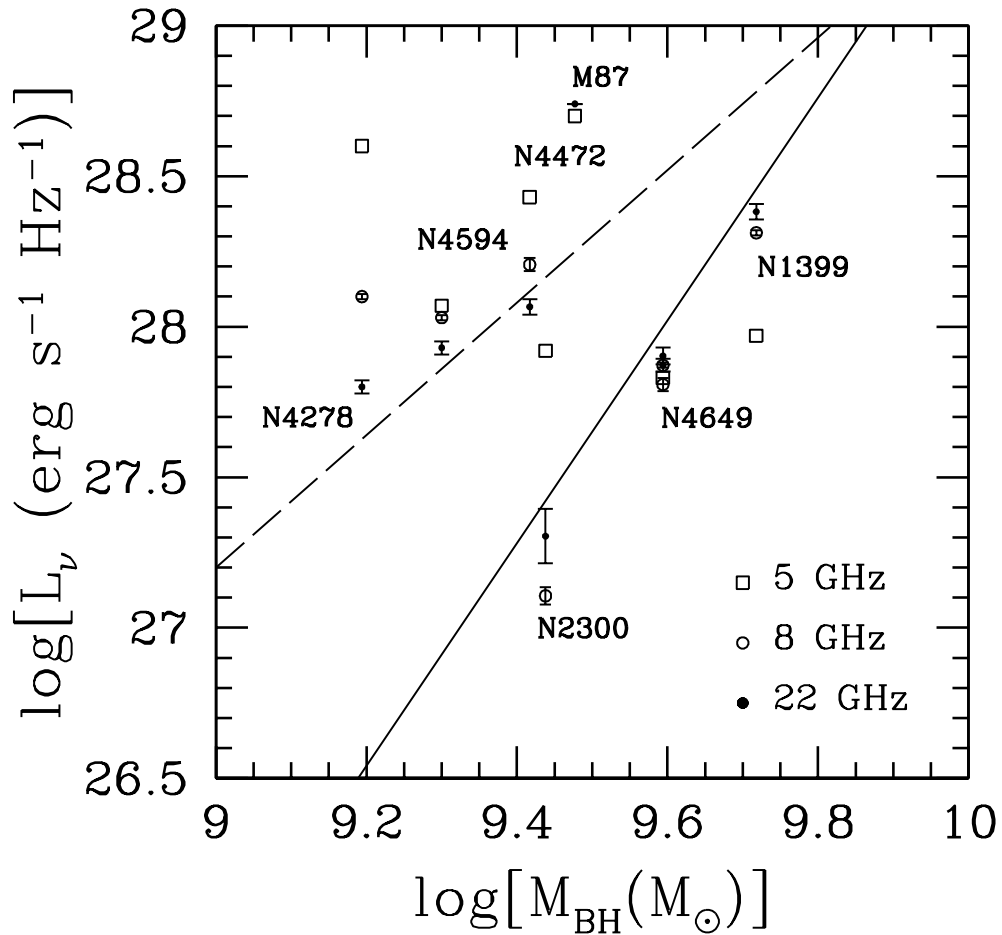


Fig. 4.— The core radio power at different frequencies. The dashed lines correspond to the ADAF based relationship $L \propto M_{BH}^{2.2}$ the solid line to ADAF + winds with $L \propto M_{BH}^{3.6}$.

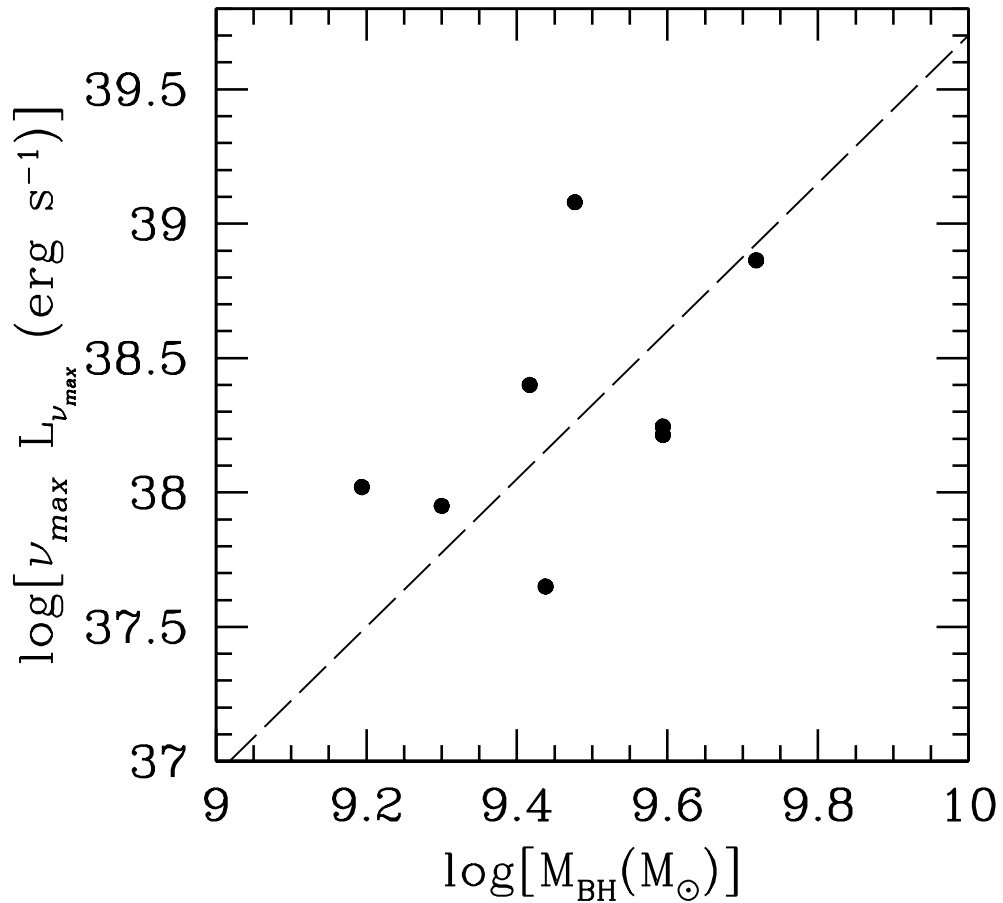


Fig. 5.— The peak radio luminosity as a function of black hole mass. The same objects as in Figure 4 are plotted. The solid lines is the relationship expected if the radio jets heat the ISM.